THE JOURNAL OF PHYSICAL CHEMISTRY B

Article

pubs.acs.org/JPCB

Bienzyme-Functionalized Monodispersed Biocompatible Cuprous Oxide/Chitosan Nanocomposite Platform for Biomedical Application

Jay Singh,[†] Manish Srivastava,[‡] Appan Roychoudhury,[§] Dong Won Lee,[†] Seung Hee Lee,[†] and B. D. Malhotra*[,∥,⊥]

[†]Department of BIN Fusion Technology and Department of Polymer-Nano Science and Technology, Chonbuk National University, Jeonju, Jeonbuk 561-756, Korea

[‡]Department of Physics, Motilal Nehru National Institute of Technology, Allahabad, Allahabad 211004, India

[§]Department of Science & Technology Centre on Biomolecular Electronics, Biomedical Instrumentation Section, Material Physics and Engineering Division, National Physical Laboratory, (CSIR), Dr. K.S. Krishnan Marg, New Delhi, 110012, India

[∥]Department of Biotechnology, Delhi Technological University, Shahbad Daulatpur, Main Bawana Road, Delhi, 110042, India

[⊥]Centre for NanoBioengineering & Spintronics, Chungnam National University, 220 Gung-Dong,Yuseon-Gu, 305-764, Deajeon, Korea

Supporting Information

ABSTRACT: The ultrafine monodispersed cuprous oxide (Ufm-Cu_2O) nanoparticles have been successfully synthesized by a facile wet chemical method using poly-*N*-vinylpyrrolidone (PVP) as a capping agent. This colloidal solution of Ufm-Cu_2O and chitosan (CS) is electrophoretically deposited (EPD) onto the indium tin-oxide (ITO) glass substrate. Thus synthesized nanocomposite has been characterized by X-ray powder diffraction (XRD, ~6 nm), scanning electron microscopy (SEM), transmission electron microscopy (TEM), and Fourier transform infrared (FTIR) spectroscopic techniques. This novel biomedical nanocomposite platform has been explored to fabricate a cholesterol biosensor by immobilizing cholesterol esterase (ChEt) and cholesterol oxidase (ChOx) onto Ufm-Cu_2O-CS/ITO electrode surface. The seed germination tests of these biomaterials (Ufm-Cu_2O-CS nanocomposite and ChOx-ChEtUfm-CuO_2-CS nanobiocomposite), conducted using the disc diffusion method, reveal strong activity against the common pathogens and crops, indicating biocompatibility of the nanocomposite. Under optimized conditions, the linearity between the current response and the cholesterol concentration has been obtained in the range of 10−450 mg/dL, with detection limit of 15.9 mg/dLcm^{-2} and a high sensitivity of 0.895 μA/(mg/dLcm^{-2}). The proposed biocompatible ChEt-ChOx/Ufm-Cu_2O-CS/ITO bioelectrode shows fast response time (<5 s), good reproducibility, and long-term stability. This biocompatible biosensor has been used to determine the total cholesterol levels in human serum samples. Investigated antimicrobial activities of bienzyme-functionalized Ufm-Cu_2O-CS nanocomposite are the potential platform for biomedical applications.

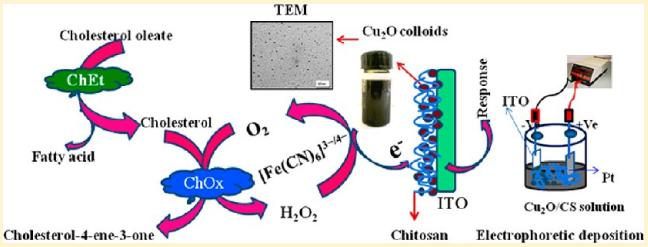

INTRODUCTION

Cholesterol is known to be an important biomolecule because it is used in our bodies for the production of hormones, bile acids, and vitamin D and is an important constituent of cell membranes. Besides this, it is an important indicator for the onset of heart disease.[1] The reliable and fast determination of cholesterol is thus extremely important for a number of applications including those in biotechnology, clinical diagnostics, and food industry.[2−5] With this in view, efforts are being made to develop biomedical devices that can be used for the estimation of cholesterol in desired test specimens. The development of biosensors for clinical diagnostics has aroused much attention. In this context, electrochemical biosensors have been considered to provide a reliable approach for rapid assay of cholesterol in the biological fluids due to rapid response, simplicity, and low cost.[6−8] Many biomaterials such as metals (e.g., gold), polymers (conducting and nonconducting), and nanomaterials (metal oxides, quantum dots, carbon nanotubes) have been found to result in improved stability of the biosensing molecules such as cholesterol esterase, cholesterol oxidase, and peroxidase, which are integral components of a cholesterol biosensor.[9−13]

The nanostructured materials with different sizes and shapes have been utilized as the substrates for immobilization of desired enzymes.[14−16] It has been demonstrated that the enzymes immobilized onto nanostructured materials have many advantages over bulk solid substrates.[17] In this context, nanoparticles of the coinage metals and their oxides have

Received: September 28, 2012
Revised: November 29, 2012
Published: December 27, 2012

attracted much attention due to their fascinating optical, electronic, catalytic, and charge-transfer ability toward the biomolecules onto a given substrate,[18,19] and as a p-type semiconductor (direct band gap as 2.17 eV) with unique optical and magnetic properties, cuprous oxide (Cu_2O) has been found to be a promising material with potential applications in solar energy conversion, micro/nanoelectronics, magnetic storage devices, biosensing, and catalysis.[20−24] The Cu_2O is known to be an interesting and facile electrode material with high efficiency for detection of biomolecules.[24,25] It has been observed that the morphology, shape, size, dispersibility, and surface conditions are important factors that may influence the electron-transport mechanism of a nanomaterial, and consequently they play a crucial role in the operation of efficient and highly sensitive electrochemical sensors.[26−28] These electronic transducers reduce the pathway for electron communication between redox biomolecules to the electrode for sensitive and speedy detection of desired analytes without any hindrance. Therefore, extensive efforts are being made to synthesize novel nanosized materials. Because of extreme smallness of these nanomaterials, it is possible to pack the number of biomolecule-functionalized nanomaterials onto an array device. Furthermore, the enhanced electrochemistry is due to the ability of the ultrafine nanoparticles to decrease the distance between the redox site of a protein and the electrode because the rate of electron transfer is inversely dependent on the exponential distance between them. Therefore, novel nanomaterials with control of size, shape, and structure can be tuned via physical, chemical, and biological routes.[27,29]

Biocompatibility is an important prerequisite for the construction of a biosensor. In general, adsorption of the desired biomolecules directly onto naked surfaces of bulk materials may result in their denaturation and loss of bioactivity. However, adsorption of such biomolecules onto the surfaces of ultrafine nanoparticles may perhaps result in the retention of the bioactivity because of biocompatibility of the nanoparticles. Because most of the nanoparticles carry high isoelectric point (>IEP), they can electrostatically adsorb enzymes with different charges with the low IEP of enzymes or proteins. Recently, many scientists including biologists have focused on the preparation of newer nanocomposites with good biocompatibility that could be the promising matrices for enzyme immobilization, which, in turn, may result in enhanced selectivity and sensitivity of the given biosensors. Among the natural biocompatible macromolecules, chitosan (CS) is a biodegradable polymer obtained from marine versatile biopolymer-chitin. Its excellent film-forming ability, biocompatibility, good adhesion, and high mechanical strength have led to growing interest in immobilizing biomolecules in recent years.[30,31] Chitosan can accumulate metal ions through various mechanisms, such as chelation, electrostatic attraction, and ion exchange, depending on the nature of the metal ion and pH of the solution.[11]

The orientation and immobilization of desired enzymes are important parameters that play important roles toward the performance of a biosensor. The immobilized biomolecules should have an appropriate orientation to facilitate communication between active center of the biomolecules and the electrode surface. The transfer of electrons generated during a biochemical reaction strongly depends on the immobilization procedure. Several methods including physical adsorption, entrapment in a dialysis membrane or within a polymeric film, covalent coupling, and cross-linking can be used to immobilize an enzyme onto the electrode surface.[32,33] These methods may lead to the formation of a randomly oriented layer, either on the surface of an electrode or in the cavities formed as a result of porosity of the matrix. However, the randomly oriented enzyme layers may affect electron communication between a biomolecule and the electrode. The design of a suitable surface to obtain anisotropic immobilization of enzymes is important for enhancing the performance of a biosensor. A variety of synthesis processes have been proposed for the deposition of thin films of nanomaterials and nanocomposites on the conductive electrode surfaces for the fabrication of electrochemical biotransducers. Among these, electrophoretic deposition (EPD) technique is known to yield uniform, dense, and porous films with advantages of the reduced processing time and simple experimental design. In particular, as a wet process, EPD provides easy control of thickness and morphology of the deposited film by tailoring various parameters such as deposition time, applied potential, and so on.[34,35]

The present article relates to results of the studies relating to the development of a biocompatible amperometric cholesterol biosensor based on ChEt and ChOx with a high sensitivity and a wide range of linearity for the rapid measurement of total cholesterol in complex biological fluids such as human whole blood. We describe a facile method to prepare monodispersed Cu_2O nanoparticles mixed with chitosan matrix using EPD onto the glass substrate. The optimized experimental conditions for fabrication and operation of the cholesterol biosensor have been established. The resulting biosensor can be used for total cholesterol in clinical samples.

MATERIALS AND METHODS

Materials. Copper sulfate ($CuSO_4{\cdot}5H_2O$), poly-*N*-vinylpyrrolidone (PVP, MW, <50000), sodium borohydride ($NaBH_4$), ethylene glycol (EG, $C_2H_6O_2$) and sodium hydroxide pallets (NaOH) have been purchased from MERC (New Delhi, India). Chitosan powder (85% deacetylation, low molecular weight), cholesterol oxidase (EC 1.1.36 from *Pseudomonas fluorescens* with specific activity of 26.4 U mg^{-1}), cholesterol esterase (EC 232.808.6 from *Pseudomonas fluorescens* with specific activity of 13.13 U mg^{-1}), horseradish peroxidise (HRP, 316Umg^{-1}), *O*-dianisidine (1%) dye, cholesterol oleate ($C_{45}H_{78}O_2$), and Brij solution (polidocanol) have been procured from Sigma−Aldrich (USA). The stock solutions of ChOx and ChEt (2 mg/mL) and HRP are freshly prepared in phosphate buffer (50 mM, pH 7.0). The cholesterol oleate solution is prepared in 1% brij solution (polidocanol) prior to use and is stored at 4 °C. The indium tin oxide (ITO)-coated glass (Balzers) sheet of resistance 15 W/cm is used as the substrate for deposition of the desired nanocomposite and as the working electrode. All solutions in these studies have been prepared with deionized water of resistivity not less than 18 MΩ cm taken from a Milli-Q water purification system (Milli-Q, USA).

Characterization. The cyclic voltammetry (CV), electrochemical impedance spectroscopy (EIS), and amperometric measurements were recorded on an Autolab Potentiostat/Galvanostat (Eco Chemie, The Netherlands). The electrochemical measurements were conducted on a three-electrodes system with ChEt-ChOx/Ufm-Cu_2O-CS/ITO bioelectrode as the working electrode, a platinum (Pt) wire as the counter electrode, and saturated Ag/AgCl electrode as a reference electrode in phosphate buffer saline (50 mM, pH 7.0, 0.9% NaCl) containing 5 mM $[Fe(CN)_6]^{3-/4-}$ as a mediator. Fourier

dx.doi.org/10.1021/jp309639w | J. Phys. Chem. B 2013, 117, 141−152

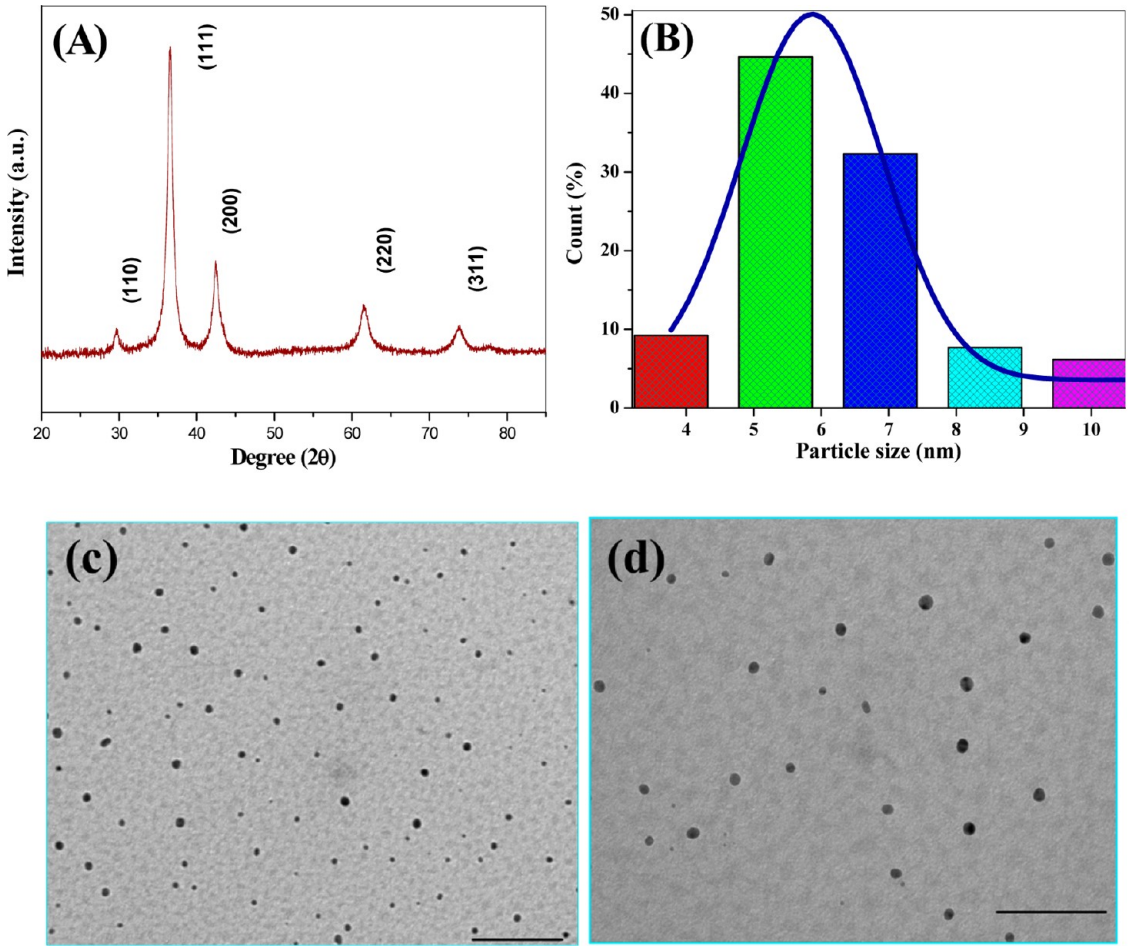

Figure 1. (A) X-ray diffraction pattern of Cu_2O nanoparticles. (B) Size distribution histograms and Gaussian fits for Cu_2O nanoparticles. (C) TEM images of ultrafine monodispersed Cu_2O nanoparticles. Scale bar corresponds to 50 nm.

transform infrared (FTIR) spectrophotometer (PerkinElmer, Spectrum BX II) was characterized in the range 400−4000 cm^{-1}. The UV−visible spectroscopic studies were conducted using a UV/vis/NIR spectrometer (PerkinElmer, Lamda 950). Phase/crystalline features of the synthesized sample were probed by X-ray powder diffraction (XRD) using a Philips X'Pert Pro diffractometer with Cu Kα radiation (λ = 1.54060 Å). Particle size and shape investigation were done through transmission electron microscope (TEM) measurements (Hitachi Model H-800 instrument) having a tungsten filament at an accelerating voltage of 200 kV. The surface morphological studies of CS/ITO film, Ufm-Cu_2O-CS/ITO film, and ChEt-ChOx/Ufm-Cu_2O-CS/ITO-modified bioelectrodes were investigated using a scanning electron microscope (LEO-440).

Preparation of Cu_2O Colloidal Solution and Cu_2O Nanoparticles. The ultrafine monodispersed Cu_2O (Ufm-Cu_2O) nanoparticles in organic solvent have been prepared as follows. A 0.5 g of poly(*N*-vinylpyrrolidone) (PVP, MW = 55 000), acting as the capping agent, was dissolved in 20 mL of EG in a flask. Afterward, at room temperature, copper(II) sulfate (5 mL of a 0.1 M solution in distilled water) was added under strong magnetic stirring, followed by adjusting the solution pH up to ~11 with dropwise addition of 1 M NaOH-EG solution. Furthermore, 3 mL of 0.5 M solution of $NaBH_4$ was quickly added to the round-bottomed flask with vigorous magnetic stirring. Within a few minutes, the deep-blue solution gradually became colorless; then, it turned burgundy, indicating the formation of Cu_2O colloid in the presence of atmospheric oxygen. The resulting colloidal was dried at 80 °C to obtain the powder form of Cu_2O sample that was used for further characterization.

Electrophoretic Deposition of Ufm-Cu_2O-CS/ITO Nanocomposite Film. EPD was carried out by using DC battery (BioRad, model 200/2.0). Typically the colloidal suspension of Ufm-Cu_2O-CS was prepared by mixing 5 mL of 1 wt % clear CS solution prepared in 0.1 M acetic acid and 2 mL of Cu_2O (10 mg/mL) colloid was diluted in DW with the ratio of 1:1 and sonicated during 30 min for proper dispersion of Cu_2O nanoparticle into CS solution prior to EPD. A voltage of 120 V for 3 min was applied to obtain thin, uniform, and homogeneous films of Ufm-Cu_2O-CS nanocomposite onto the surface of ITO-coated glass surface (0.25 cm^2) and dried for 12h at room temperature.

Immobilization of ChOx and ChEt on Ufm-Cu_2O-CS Nanocomposite Film. Freshly prepared solutions of ChOx (2 mg/mL) and ChEt (2 mg/mL) taken in the same ratio (1:1) are prepared in phosphate buffer (50 mM, pH 7.0) and uniformly spread (15 μL) onto the desired Ufm-Cu_2O-CS/ITO nanocomposite electrode. The ChEt-ChOx/Ufm-Cu_2O-CS/ITO bioelectrode was kept undisturbed in a humid chamber for ~12 h at room temperature. This bioelectrode (ChEt-ChOx/Ufm-Cu_2O-CS/ITO) was washed thoroughly with phosphate buffer (50 mM, pH 7.0) containing 0.9% NaCl to remove any unbound enzyme and stored at 4 °C when not in use.

dx.doi.org/10.1021/jp309639w | *J. Phys. Chem. B* 2013, 117, 141−152

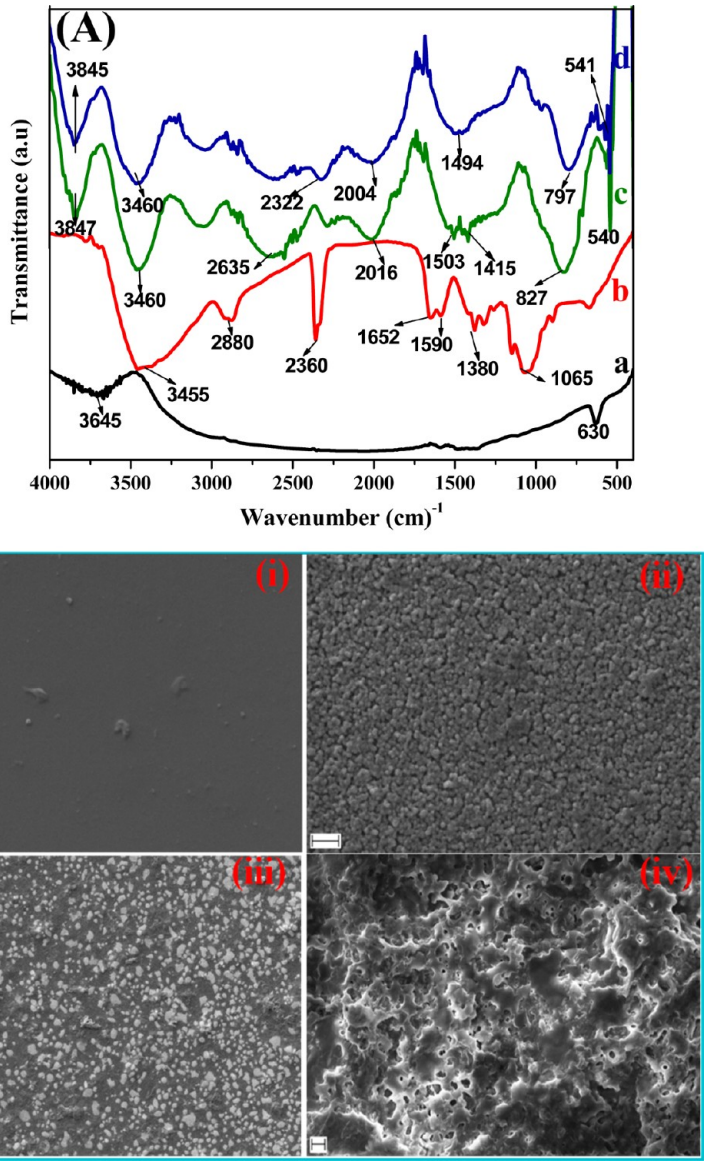

Figure 2. (A) FTIR transmission spectra of (a) Cu_2O nanoparticles, (b) CS/ITO film, (c) Ufm-Cu_2O-CS/ITO film, and (d) ChEt-ChOx/Ufm-Cu_2O-CS/ITO bioelectrodes, (B) SEM images of CS/ITO film (i), electrophoretically deposited Cu_2O nanoparticles (ii), Ufm-Cu_2O-CS/ITO film (iii), and ChEt-ChOx/Ufm-Cu_2O-CS/ITO bioelectrodes (iv). Scale bar corresponds to 1 μm.

Biocompatibility Test. The effect of Ufm-Cu_2O-CS and ChEt-ChOx/Ufm-Cu_2O-CS solution on the germination of seeds of mustard and tomato crops has been evaluated using standard germination assay. The seeds are surface-sterilized with 0.1% (v/v) mercuric chloride for 30 min, washed with DW, and soaked in water overnight and are kept in the incubator at 17 and 24 °C, respectively. Five mL of 1.2% water agar is poured as medium in each well of 12 wells plates. Three seeds are kept in each well for the each treatment. Ten μL of the CS, Ufm-Cu_2O-CS, and ChEt-ChOx/Ufm-Cu_2O-CS solution is used for the testing. Distilled water is used as a control for each plate. The plates of mustard and tomato seeds are kept in an incubator at 17 and 24 °C, respectively. Observations are taken regularly up to 72 h incubation period.

RESULTS AND DISCUSSION

Growth Process and Possible Growth Mechanism. It is expected that during the growth process, the formation of $Cu(OH)_2$ is catalyzed by complexation of Cu^{2+} ion by polypyroledinone (PVP) molecules. PVP might play a role for preventing the aggregation of $Cu(OH)_2$ precursor for the formation of colloidal Cu_2O nanoparticles. Moreover, the spherical shape of Cu_2O nanoparticles is due to reduced surface energy because of steric effect of PVP molecules.[36] During the synthesis, dropwise addition of NaOH-EG solution into the pale-blue solution of $CuSO_4{\cdot}5H_2O$ results in the initial formation of a white blue precipitate likely to be attributed for the formation of $Cu(OH)_2$/PVP complex. Then, this precipitate gradually dissolves and turns into a deep-blue clear solution with further addition of NaOH-EG to reach pH 11. It has been suggested that hydroxide ions and EG may coordinate with Cu^{2+} by replacing the PVP molecule. An intermediate Cu(II)-hydroxyl-EG complex may form at this stage before it is reduced by $NaBH_4$. Furthermore, the addition of $NaBH_4$-EG solution first turns the deep-blue solution into nearly colorless and eventually to burgundy, confirming the formation of Cu_2O(I) nanoparticles.[37] Monodispersed Cu_2O particles are synthesized by the solution-phase reaction between Cu(II)-

dx.doi.org/10.1021/jp309639w | J. Phys. Chem. B 2013, 117, 141−152

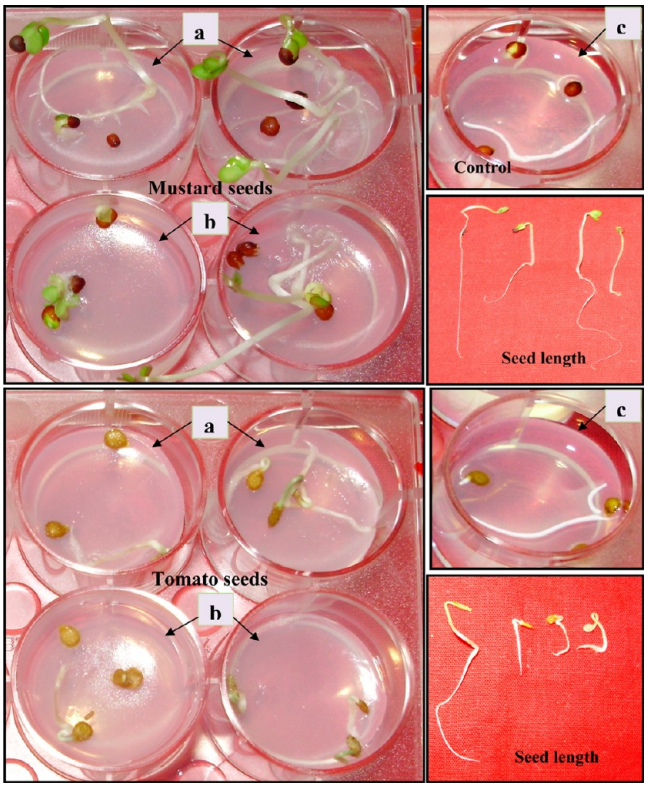

Figure 3. Snapshot of the seed (mustard and tomato) germination in the plant culture using Cu_2O-CS (A) and ChEt-ChOx/Cu_2O-CS (B) and control (C) solution (0.1%) seeds after 4 days of incubation, revealing proper seed germination, showing biocompatibility of Cu_2O-CS and ChEt-ChOx/Cu_2O-CS nanocomposite solution.

Table 1. Bioassay of Cu_2O/CS (A) ChEt-ChOx/Ufm-Cu_2O/CS (B) and Control (C) against Tomato and Mustard Seeds[a]

		seeds			
		mustard		tomato	
s. no.	sample	% germination	seedling length	% germination	seedling length (cm)
1	A	83.33	8.7	33.33	3.05
2	B	66.66	4.75	49.995	2.6
3	C	49.995	9.05	49.995	2.25

[a]Observations: After 48 h; 10 μL samples were used; average of five seeds in replicates.

hydroxyl-EG complex and $NaBH_4$-EG solution that act as a strong reducing agent and reduce copper hydroxide to cuprous oxide at ~80 °C. The possible chemical reactions can be given as follows:

$$CuSO_4{\cdot}5H_2O \rightarrow Cu^{2+} + SO_4^- \quad \text{(i)}$$

$$Cu^{2+} + 2NaOH \rightarrow Cu(OH)_2 + 2Na^+ \quad \text{(ii)}$$

$$Cu(OH)_2 \rightarrow Cu^{2+} + 2OH^- \quad \text{(iii)}$$

$$4Cu^{2+} + BH_4^- + 5H_2O \xrightarrow{80^\circ C} Cu_2O + B(OH)_3 + 2H_2 + 7H^+ \quad \text{(iv)}$$

Structural and Morphological Studies. Figure 1A shows the XRD pattern of Ufm-Cu_2O nanoparticles. All diffraction peaks have been indexed at (110), (111), (200), (220), and (311) corresponding to cubic-phase Cu_2O, which agree well with JCPDS 05-0667. The value of lattice constant (a) has been calculated to be 4.278 Å. Moreover, no other peak is observed in the XRD pattern, which also confirms the formation of impurity-free Cu_2O phase. The average grain size has been calculated by using the Debye−Scherrer formula, and it turned out to be ~8 nm.[38]

The shape and size of the Cu_2O nanoparticles have been investigated using TEM, as shown in Figure 1c,d. TEM images show that the nanoparticles are monodispersed and spherical in shape and are uniformly distributed without aggregation. The average size of the particles was calculated through the particle size distribution curve and has been found to be ~6 nm Figure 1B.

The FT-IR spectra of Ufm-Cu_2O nanoparticles, CS/ITO film, Ufm-Cu_2O-CS/ITO, and ChEt-ChOx/Ufm-Cu_2O-CS/ITO bioelectrodes are shown in Figure 2A in the range 400−4000 cm^{-1}. The FTIR spectra of Ufm-Cu_2O nanoparticles (curve a) exhibit broad bands at 3645 cm^{-1} corresponding to O−H stretching due to physically adsorbed water and characteristic absorption bands at 630 cm^{-1}, confirming that the synthesized product has Cu_2O phase only. In the case of the CuO phase, four oxygen atoms are linked with the Cu atom in a square planar geometry, whereas in the case of Cu_2O, two oxygen atoms are connected together with a linear coordination. Therefore, Cu(II)-O bonds in CuO are weaker than Cu(I)-O bonds in Cu_2O, and thus the vibration of Cu−O bond in the CuO phase exists at a lower frequency than that of the Cu−O bond in Cu_2O phase.[39] The FTIR spectrum (curve b) of CS/ITO electrode exhibits characteristic absorption bands of amino saccharide at 3455 cm^{-1} arising due to overlapping of −OH and $-NH_2$ bands. The peaks seen at 2923 and 2880 cm^{-1} are due to CH_2 stretching, and peaks found at 1652 and 1590 cm^{-1} are for carbonyl stretching (C═O) of amide I and amide II groups. The peak seen at 1380 cm^{-1} is assigned to the −C−O stretching mode of $-CH_2-OH$ groups, and the broad peak, seen at 1065 cm^{-1}, is assigned to the β (1−4) glucosidic band in the polysaccharide unit. Furthermore, the peaks seen at 1080 to 1020 cm^{-1} are attributed to the stretching vibration mode of the hydroxyl group and C−O−C in glucosamine unit.[31] The FTIR spectra of the Ufm-Cu_2O-CS/ITO film (curve c) exhibits characteristic IR bands of the functional group corresponding to pure CS (curve b), and additional bands found at 540 and 827 cm^{-1} indicate the formation of the M-O band. This suggests that the M-O-M inorganic network is bonded with the CS macromolecules via both hydrogen bonding and ionic bonding in the Ufm-Cu_2O/ITO electrode. However, ChEt-ChOx/Ufm-Cu_2O-CS/ITO bioelectrode (curve d) shows broadening of the peak at 3845 and 3460 cm^{-1} due to the addition of −OH and $-NH_2$ groups of CS. The broad band seen at 1494 cm^{-1} corresponding to C−N stretching and N−H bending modes of amide I bands and 1063 cm^{-1} are assigned to C−O stretching due to amide bands in protein, revealing immobilization of enzymes onto Ufm-Cu_2O-CS/ITO nanocomposite matrix via electrostatic interactions.

Surface morphological studies of CS/ITO film, Ufm-Cu_2O nanoparticles, Ufm-Cu_2O-CS/ITO, and ChEt-ChOx/Ufm-Cu_2O-CS/ITO bioelectrodes investigated using scanning electron microscopy (SEM) are shown in Figure 2B. The CS/ITO film (image i) shows homogeneous, with relatively smooth, mesoporous and crack-free surface. The SEM image of Ufm-Cu_2O nanoparticles (image ii) exhibits homogeneous

dx.doi.org/10.1021/jp309639w | J. Phys. Chem. B 2013, 117, 141−152

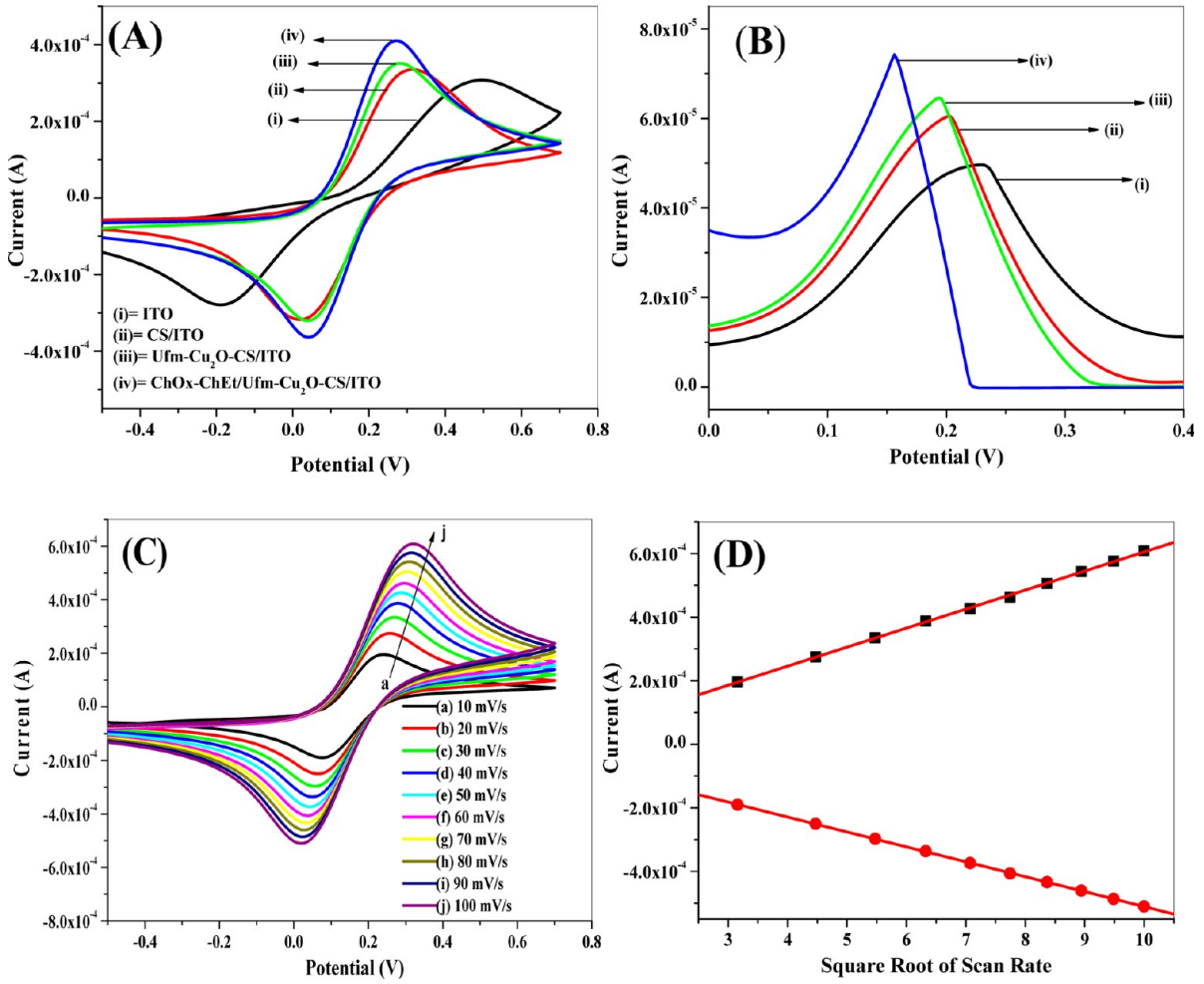

Figure 4. (A) CV and (B) DPV of a bare ITO electrode (a), the CS/ITO electrode (b), the Ufm-Cu_2O-CS/ITO electrode (c), and the ChEt-ChOx/Ufm-Cu_2O-CS/ITO bioelectrode (d). (C) CV of the ChEt-ChOx/Ufm-Cu_2O-CS/ITO bioelectrode using an increasing scan rate of 10 to 100 mV/s. (D) Magnitude of current versus potential difference as function of square root of scan rate (10−100 mV/s).

distribution of very fine spherically shaped particles, with a mean diameter of 50−70 nm. It appears that nanoparticles perhaps agglomerate due to high surface charge. The SEM image of Ufm-Cu_2O-CS/ITO film (image iii) shows granular and spherical nanoporous morphology embedded uniformly in the porous CS matrix with minimum aggregation. It appears that CS perhaps bridges the individual Cu_2O particles. However, on the immobilization of ChEt and ChOx, the granular and fibril spherical morphology of Ufm-Cu_2O-CS/ITO film changes into the homogeneous globular porous morphology due to ionic interactions between Ufm-Cu_2O nanoparticle and biomolecules, indicating immobilization of enzymes (image iv). Moreover, this globular and porous network of Ufm-Cu_2O-CS/ITO film provides increased surface area for immobilization of biomolecules resulting in high enzyme loading.

Biocompatibility and Antimicrobial Activity Studies. The observations pertaining to the effect of Ufm-Cu_2O-CS and ChEt-ChOx/Ufm-Cu_2O-CS on mustard and tomato seed germination shown in Figure 3a,b, respectively, reveal appropriate seed germination of the plant tissue culture, indicating biocompatible nature of the nanocomposite. The germinated seeds have been counted for each treatment and expressed as % germination (Table 1). The length of germinated seedlings is measured and compared for each treatment. All treatments are taken in triplicate.

The antimicrobial studies have been conducted by investigating the development of inhibition zone regularly up to 72 h incubation period in different algal/fungal/bacterial strains shown in the Supporting Information (Figure S1). The retardation of inhibition zone is taken as the positive sign indicating biosafety of the Ufm-Cu_2O-CS-modified bioelectrode on the microorganisms culture, which is shown in the Supporting Information (Table S1).

Electrochemical Studies, Cyclic Voltammetry Studies. Figure 4A shows the typical CV sweep curve of bare ITO, CS/ITO, Ufm-Cu_2O-CS/ITO, and ChEt-ChOx/Ufm-Cu_2O-CS/ITO bioelectrode, respectively, in PBS (50 mM, pH 7.0, 0.9% NaCl) containing $[Fe(CN)_6]^{3-/4-}$ (5 mM) at 30 mV/s scan rate. The CV of bare ITO (curve i) exhibits a well-defined electrochemical characteristics with a couple of redox peaks for $[Fe(CN)_6]^{3-/4-}$ mediator and shows oxidation peak current (I_{pa}) at 0.3 mA. After modification with CS, the oxidation peak current (I_{pa}) increases to 0.33 mA (curve ii) due to the cationic nature of CS that is favorable for the interaction with ferro and ferricyanide ions. On incorporation of Ufm-Cu_2O nanoparticles into the CS matrix, the I_{pa} (0.35 mA) is found to increase for Ufm-Cu_2O-CS/ITO electrode (curve iii) due to high electrocatalytic ability, increased surface area, and high surface energy

dx.doi.org/10.1021/jp309639w | J. Phys. Chem. B 2013, 117, 141−152

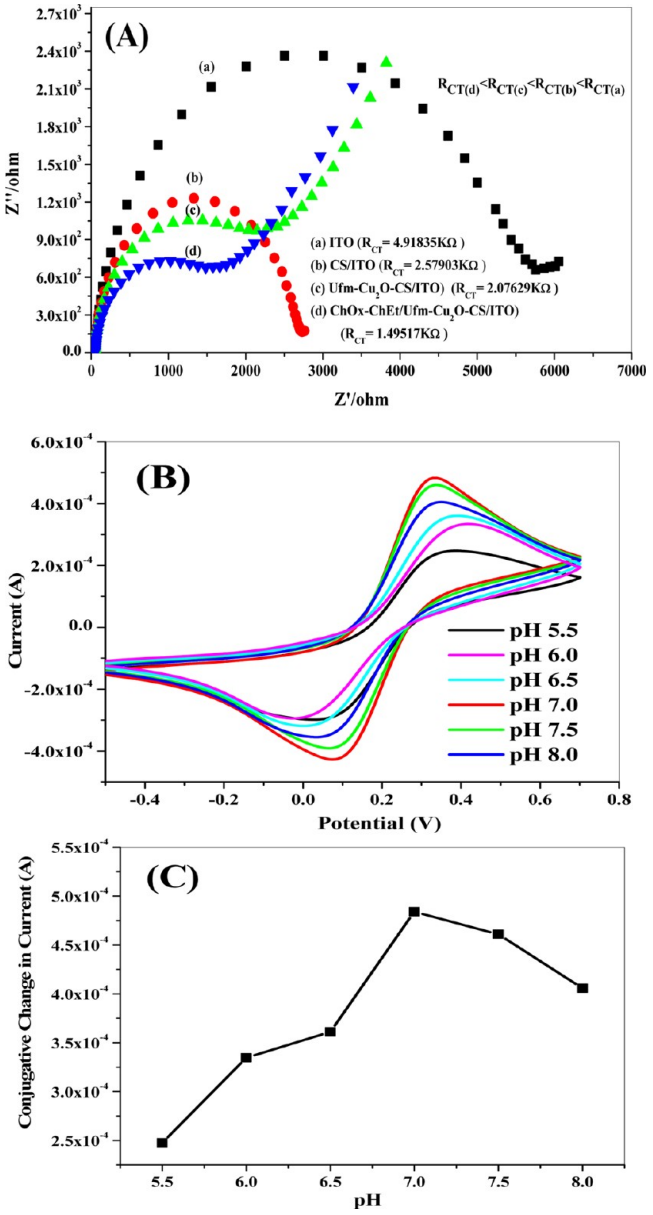

Figure 5. (A) EIS of bare ITO electrode (a), CS/ITO electrode (b), the Ufm-Cu_2O-CS/ITO electrode (c), and the ChEt-ChOx/Ufm-Cu_2O-CS/ITO bioelectrode (d). (B) CV studies of the ChEt-ChOx/Ufm-Cu_2O-CS/ITO bioelectrode as a function of pH (ranging from 5.8 to 8.0 in phosphate buffer containing $[Fe(CN)_6]^{3-/4-}$. (C) Change in current response as a function the ChEt-ChOx/Ufm-Cu_2O-CS/ITO bioelectrode pH.

of Cu_2O nanoparticles that fascinate electron transfer. The magnitude of I_{pa} further increases to 0.41 mA (curve iv) after immobilization of ChEt and ChOx enzymes onto the Ufm-Cu_2O-CS/ITO electrode surface because it provides a suitable native environment for the immobilization of enzymes and Ufm-Cu_2O nanoparticles that catalyze and promote electron communication between the enzymes and Ufm-Cu_2O-CS/ITO electrode. The results of differential pulse voltammetric (DPV) studies reveal similar behavior of the redox potential toward the Cu_2O-modified electrode shown in the Figure 4B.

Figure 4C exhibits CV spectra of ChEt-ChOx/Ufm-Cu_2O-CS/ITO bioelectrode in PBS (pH 7.0) as a function of scan rate varying from 10 to 100 mV/s. As shown in the Figure 4D, the magnitudes of cathodic (I_{pc}) and anodic (I_{pa}) peak currents increase linearly with square root of scan rate ($\upsilon^{1/2}$), indicating a typical diffusion controlled electrochemical behavior, and it depends on the value of diffusion coefficient. Moreover, the potential peak shift ($\Delta E_p = E_{pa} - E_{pc}$) exhibits a linear relationship (linear regression coefficient of 0.9901) with scan rate shown in Supporting Information (Figure S2), suggesting improved electrocatalytic behavior.

The diffusion coefficient value (D) or diffusion of charge in matrix of ChEt-ChOx/Ufm-Cu_2O-CS/ITO bioelectrode has been calculated using the Randles−Sevcik equation.[11]

$$I_p = (2.69x10^5)n^{3/2}AD^{1/2}CV^{1/2} \quad \text{(v)}$$

where I_p is the peak current of the bioelectrode (I_{pa} and I_{pc}), n is the number of electrons involved or electron stoichiometry (1), A is the surface area of the bioelectrode (0.25 cm^2), D is the diffusion coefficient, C is the surface concentration in mol (0.322025×10^{-10} mol), and V is the scan rate (30 mV/s). The D value is obtained as 2.5×10^{12} cm^2 s^{-1}.

The surface concentration of the electrodes has been estimated using the Brown−Anson model by following equation.[11]

$$Ip = n^2F^2I^*AV/4RT \quad \text{(vi)}$$

where n is the number of electrons transferred (1), F is the Faraday constant (96485 C/mol), I^* is the surface concentration of the corresponding electrode (mol cm^{-2}), A is the surface area of the electrode (0.25 cm^2), V is the scan rate (30 mV/s), R is the gas constant (8.314 J mol^{-1} K^{-1}), and T is the room temperature (300 K). The surface concentration of ChEt-ChOx/Ufm-Cu_2O-CS/ITO (8.79×10^{-11} mol cm^{-2}) is higher than that of Ufm-Cu_2O-CS/ITO (7.54×10^{-11} mol cm^{-2}) and CS/ITO (7.21×10^{-11} mol cm^{-2}).

Electrochemical Impedance Spectroscopy Studies. The EIS studies have been carried out to characterize the impedance change of the electrode surface in the modification process. In EIS, the semicircle diameter equals the interface electron-transfer resistance (R_{ct}), which controls the electron-transfer kinetics of the redox probe at the electrode interface. The linear part of low-frequency region corresponds to the diffusion process. Figure 5A represents impedance spectra of bare ITO, CS/ITO, Ufm-Cu_2O-CS/ITO, and ChEt-ChOx/Ufm-Cu_2O-CS/ITO electrode in PBS (50 mM, pH 7.0, 0.9% NaCl) containing $[Fe(CN)_6]^{3-/4-}$ (5 mM) in the frequency range of 0.00 to 10^7 Hz, obtained from Nyquist plot. In the Nyquist plot, charge-transfer resistance (R_{CT}) of surface-modified electrode can be estimated from diameter of the semicircular portion in the high-frequency range. It is found that charge-transfer resistance for bare ITO (R_{CT} = 4.92 KΩ, curve a) decreases for the CS/ITO electrode (R_{CT} = 2.58 KΩ, curve b), and it further decreases for the Ufm-Cu_2O-CS/ITO electrode (R_{CT} = 2.08KΩ, curve c). These results suggest that Ufm-Cu_2O-CS/ITO electrode results in improved electron transfer in between solution and the electrode and Ufm-Cu_2O nanoparticles due to permeable structure of CS/ITO electrode. On immobilization of ChEt and ChOx onto Ufm-Cu_2O-CS/ITO nanocomposite electrode, charge-transfer resistance of the bioelectrode further decreases (R_{CT} = 1.49KΩ, curve d). This observation suggests that the Ufm-Cu_2O-CS/ITO surface provides for a favorable microenvironment for enzyme immobilization resulting in high electron pathways between

dx.doi.org/10.1021/jp309639w | J. Phys. Chem. B 2013, 117, 141−152

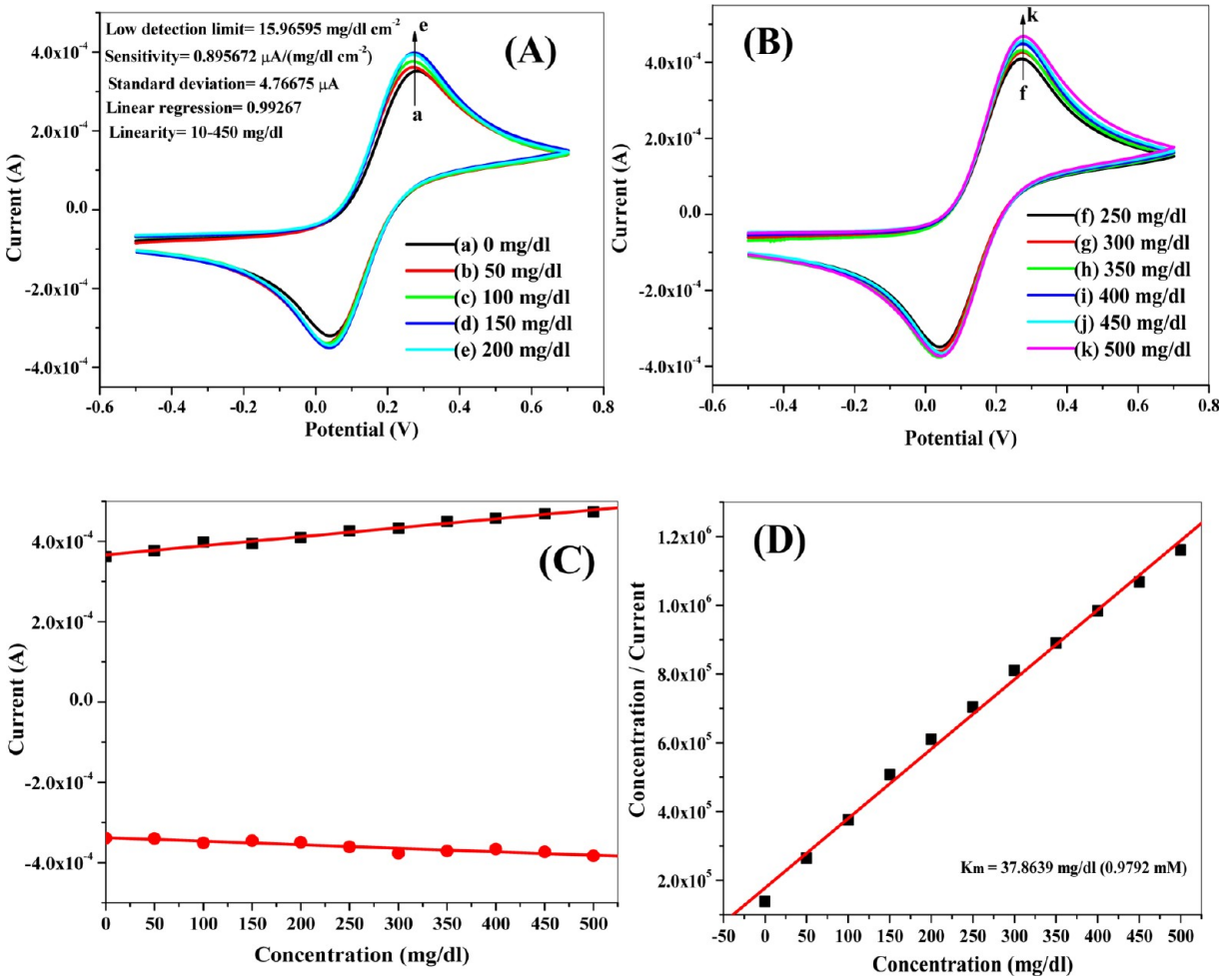

Figure 6. (A_{a-e}) and (B_{f-k}) Electrochemical response of the ChEt-ChOx/Ufm-Cu_2O-CS/ITO bioelectrode with respect to cholesterol concentration (0−500 mg/dl) in phosphate buffer containing $[Fe(CN)_6]^{3-/4-}$ at a scan rate of 30 mV/s. (C) Calibration curve and the variation in current as a function of cholesterol concentration (D) Hanes plot, which plots the substrate concentration (X axis) and substrate concentration/current (Y axis).

electrode and the electrolyte and improved diffusion of ferricyanide molecules toward the electrode surface.[40]

Influence of pH and Working Potential on the Developed Sensor Response. The effect of solution pH on the electrochemical behavior of ChEt-ChOx/Ufm-Cu_2O-CS/ITO has been investigated by CV in PBS (50 mM, pH 7.0, 0.9% NaCl) containing $[Fe(CN)_6]^{3-/4-}$ (5 mM) at 30 mV/s scan rate. As seen in Figure 5B, the redox peak current increases gradually with pH from 5.5 to 7.0, the maximum redox peak current is obtained at pH 7.0, and the E_{pa} shifts to lower values (Figure 5C). When pH further increases, the redox peak current inversely decreases and E_{pa} shifts to higher values. Therefore, pH 7.0 was chosen as the optimized condition for further investigation. It appears that the higher pH is responsible for desorption of enzyme, and the current response decreases up to 21% upon an increase in pH up to 8.0.

The effect of working potential on the performance of the bioelectrode has been investigated from 0.1 to 0.8 V in the presence of 100 μL cholesterol oleate (200 mg/dL) and a PBS (50 mM, pH 7.0, 0.9% NaCl) containing 5 mM $[Fe(CN)_6^{3-/4-}]$. The steady-state current response increases with the working potential from 0.1 to 0.3 V and then increases smoothly from 0.4 to 0.8 V shown in Supporting Information (Figure S3), which is due to the increased electron transfer. To avoid the use high working potential causing ascorbic acid and uric acid directly oxidized on the electrode surface while obtaining high sensitivity, the working potential of 0.3 V has been appropriately used.

Amperometric Response Studies of ChEt-ChOx/Ufm-Cu_2O-CS/ITO Bioelectrode. Figure 6A,B shows the amperometric response of the fabricated ChEt-ChOx/Ufm-Cu_2O-CS/ITO bioelectrode as a function of cholesterol oleate concentration (0−500 mg/dL) in PBS (50 mM, pH 7.0, 0.9% NaCl) containing $[Fe(CN)_6]^{3-/4-}$ (5 mM) at 30 mV/s scan rate using CV technique. The results show oxidation peak at 0.27 V that is attributed to enzymatic reaction between enzymes (ChEt and ChOx) and cholesterol oleate and the formation of H_2O_2. The increase in value of the oxidation current with increasing cholesterol oleate concentration (5−500 mg/dL) results in increased concentration of H_2O_2 during the enzymatic reaction. This may perhaps be due to the well-aligned cubic network of Cu_2O nanoparticles that act as a good acceptor of electrons generated during reoxidation of enzyme and transferred to electrode via Cu(I)/Cu(II) redox couple, resulting in increased electrochemical current response. As shown in the Figure 8B, the Ufm-Cu_2O-CS biocomposite film-modified electrode reaches 96% of the steady state current within 2s. The fast response can be attributed to two factors: first, the Ufm-Cu_2O nanoparticles provide not only a high surface area and excellent electrical conductivity but also

dx.doi.org/10.1021/jp309639w | J. Phys. Chem. B 2013, 117, 141−152

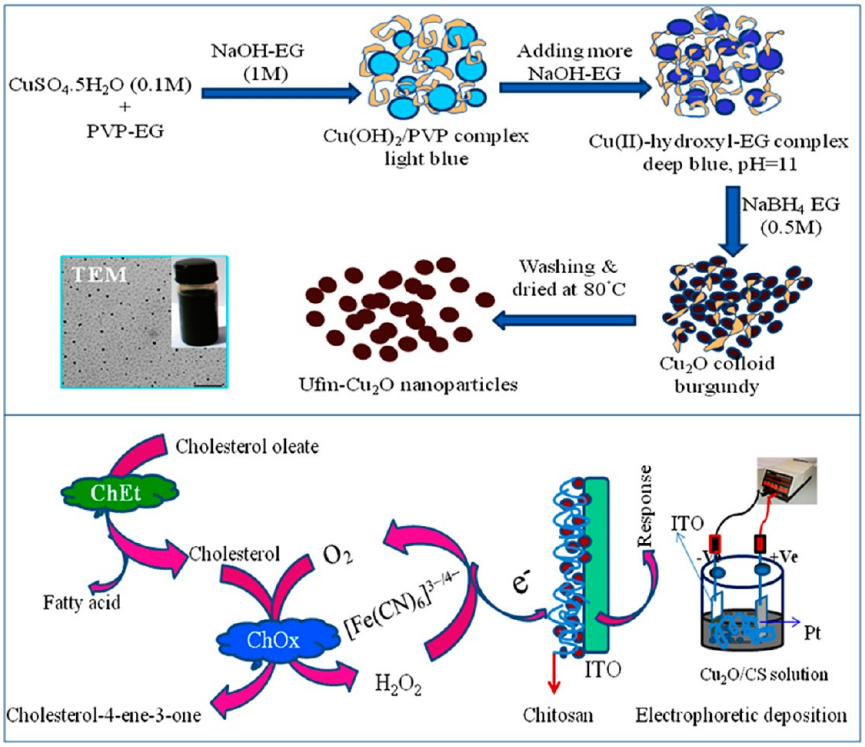

Figure 7. Schematic illustration for the possible growth of Cu_2O nanoparticles and the biochemical reaction mechanism of the immobilized ChOx and ChEt toward cholesterol.

improved electrocatalytic activity, thus allowing rapid electrooxidation of the H_2O_2; second, the CS matrix has a thin and highly porous structure, thereby facilitating fast substrate diffusion. The corresponding calibration curve (Figure 6C) shows that magnitude of the oxidation peak current increases almost linearly with increasing cholesterol oleate concentration and saturates at high concentration of cholesterol oleate. ChEt-ChOx/Ufm-Cu_2O-CS/ITO bioelectrode exhibits linear response to cholesterol oleate in the broad concentration range from 10 to 450 mg/dl with linear regression coefficient of 0.9927. The sensitivity of the fabricated bioelectrode has been calculated from the slope of the curve and obtained as 0.896 μA/(mg/dL cm^{-2}). The standard deviation and low detection limit for the bioelectrode are found to be 4.767 μA and 15.97 mg/dL cm^{-2}, respectively. Because the desired total plasma cholesterol for an individual is <5.2 mM (200 mg/dL), with a high cholesterol level being considered as greater than 6.2 mM (240 mg/dL), the fabricated biosensor covers a wide range of cholesterol concentration, promising for clinical diagnostics of total cholesterol.

The value of enzyme−substrate kinetic parameter (Michaelis−Menten constant, K_m) for the ChEt-ChOx/Ufm-Cu_2O-CS/ITO bioelectrode has been obtained as 37.86 mg/dL (0.979 mM) using Hanes plot, that is, the graph between [substrate concentration] and [substrate concentration/current] (Figure 6D). The small K_m value indicates increased affinity of ChEt-ChOx/Ufm-Cu_2O-CS/ITO bioelectrode to total cholesterol that is attributed to favorable conformation of enzymes and higher loading onto Ufm-Cu_2O-CS/ITO electrode surface. The value of K_m depends on various factors such as matrix and the method of immobilization of enzymes that may bring conformational changes in the enzyme structure as the enzyme kinetics is environment-sensitive.[41,42] It appears that biocompatible nanostructured Cu_2O-CS/ITO film results in higher activity of immobilized ChEt and ChOx molecules due to their improved conformation and orientation, leading to enhanced interaction between enzyme and substrate. This nanostructured matrix provides high electron communication between the enzyme active site and the electrode along with high surface area, providing a suitable nanoscale environment that favors immobilization of desired enzyme in a large amount on the surface of the matrix. Moreover, most of the matrices used in the development of biosensors require cross-linkers for enzyme immobilization. This is not necessary for the metal-oxide-based matrix, used in the present studies, owing to its high IEP (copper oxide ~9.5) making it suitable for bonding having low IEP of ChOx (~4.7) via physical immobilization.[43] From these results, it can be concluded that the proposed biosensor exhibits excellent performance in terms of response time, linear range, sensitivity, detection limit, and K_m. The schematic illustration for the growth of Cu_2O nanoparticles and the biochemical reaction mechanism of the immobilized ChOx and ChEt toward cholesterol are shown in Figure 7.

Photometric Enzyme Assay. The apparent enzyme activity (U cm^{-2}) is defined as one unit of enzyme activity that results in the conversion of 1 μmol of cholesterol into cholest-4-ene-3-one per minute. It can be estimated using the method based on the difference of absorbance observed before and after the incubation of enzyme-bound electrode.[44] The apparent enzyme activity has been evaluated using the following equation.

$$\alpha_{app}^{enz}(\text{U cm}^{-2}) = AV/\varepsilon ts \quad \text{(vii)}$$

where A is the difference in absorbance before and after incubation, V is the total volume (3.08 cm^3), ε is the millimolar extinction coefficient (7.5 for *o*-dianisidine at 500 nm), t is the reaction time (min), and s is the surface area (0.25 cm^2) of the electrode. For the measurement, a solution of 20 μL of HRP,

dx.doi.org/10.1021/jp309639w | J. Phys. Chem. B 2013, 117, 141−152

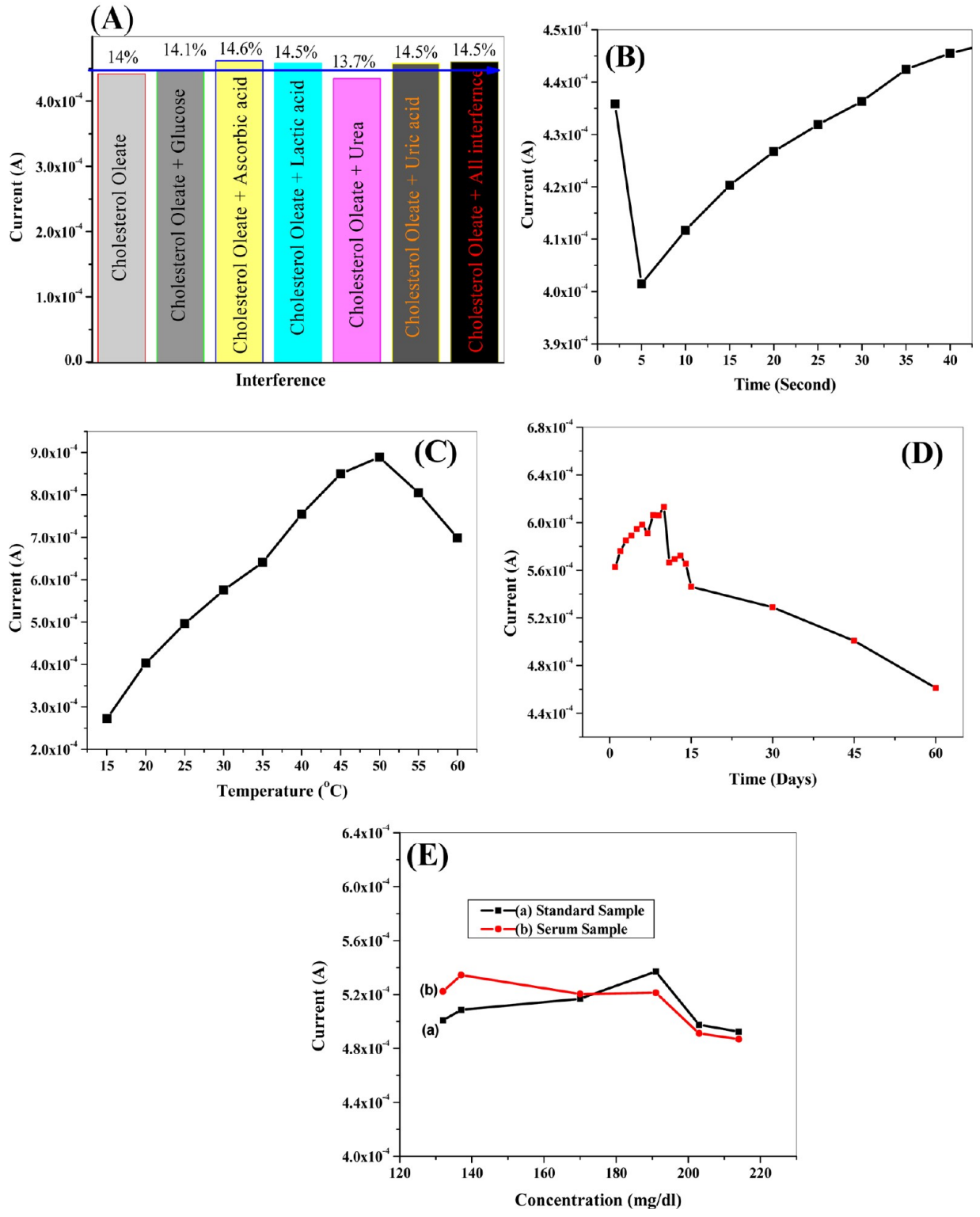

Figure 8. (A) Bar graph showing the electrctrochemical response of the ChEt-ChOx/Ufm-Cu_2O-CS/ITO bioelectrode with different interferents. (B) Electrochemical response time from 2 to 60 s of incubation period. (C) Effect of temperature on ChEt-ChOx/Ufm-Cu_2O-CS/ITO bioelectrode from 15 to 60 °C. (D) Shelf life curve for ChEt-ChOx/Ufm-Cu_2O-CS/ITO bioelectrode as a function of day. (E) Determination of cholesterol concentration: (a) prepared standard cholesterol oleate solution and (b) cholesterol concentration in serum sample.

10 μL of dye (*o*-dianisidine), and 50 μL of 100 mg dL^{-1} cholesterol oleate were diluted by adding 3 mL of PBS (pH 7.0) and it is kept in a thermostat at 25 °C. The ChEt-ChOx/Ufm-Cu_2O-CS/ITO bioelectrode is immersed and is incubated for ~3 min. This bioelectrode is then removed, and the absorbance of the solution is measured at fixed wavelength that is 500 nm using a double-beam spectrophotometer to estimate the concentration of product produced as a result of enzymatic reaction. The apparent enzyme activity has been found to be 1.538 U cm^{-2}, indicating that 1.538 units of enzyme per cm^2

dx.doi.org/10.1021/jp309639w | *J. Phys. Chem. B* 2013, 117, 141−152

Table 2. Determination of Total Cholesterol in Serum Sample

cholesterol concentration (mg/dl)	value of current obtained with serum sample (mA)	value of current obtained for pure cholesterol oleate sample (mA)	% RSD
132	0.503961	0.500027	0.79
137	0.50855	0.497405	2.24
170	0.516089	0.512483	0.70
191	0.528216	0.521333	1.32
203	0.530511	0.522644	1.51
214	0.531822	0.5292	0.50

actively participate in the enzymatic reaction. The higher activity of the immobilized enzyme is due to Ufm-Cu_2O-CS matrix with desired morphology.

Effect of Interference, Thermal Stability, Response Time, Reproducibility, and Stability of the ChOx/Ufm-Cu_2O-CS/ITO Bioelectrode. Anti-interferent behavior is an important consideration for the working of a biosensor. The influence of common interference on the fabricated ChEt-ChOx/Ufm-Cu_2O-CS/ITO bioelectrode has been determined in PBS (50 mM, pH 7.0, 0.9% NaCl) containing $[Fe(CN)_6]^{3-/4-}$ (5 mM) at 30 mV/s scan rate using CV technique shown in the Supporting Information (Figure S4). The change in electrochemical current response has been measured in PBS containing equal amount (1:1) of cholesterol oleate (100 mg/dL) as standard solution along with a normal physiological concentration of common interference such as glucose (5 mM), ascorbic acid (0.05 mM), lactic acid (0.5 mM), urea (1 mM), and uric acid (0.1 mM). The values of oxidation peak current decrease by 1.16, 4.56, 3.67, 1.6, 3.6, and 0.91% on addition of glucose, ascorbic acid, lactic acid, urea, uric acid, and mixture of these interference, respectively, shown in the bar graph of Figure 8A. These results indicate that a response of ChEt-ChOx/Ufm-Cu2O-CS/ITO bioelectrode is not significantly affected due to the presence of these interferents.

The effect of temperature on the response of the ChEt-ChOx/Ufm-Cu_2O-CS/ITO bioelectrode has been measured at temperature varying from 15 to 60 °C (Figure 8C). The reaction rate is found to increase with temperature up to 50 °C, and it then goes down as the temperature turns higher. The result shows that the immobilized enzymes get denatured after ~50 °C, and the enzyme bioconjugated with Ufm-Cu_2O nanoparticles and cover of CS film has good thermal stability.

The reproducibility of the proposed cholesterol biosensor has been investigated. Repetitive measurements have been carried out in 10 mL of PBS containing 100 mg/dL cholesterol oleate solution. The currents obtained in 15 repeated measurements show an RSD of 2 to 3%, confirming that the measured results are reproducible. The results suggest that the film of Ufm-Cu_2O-CS/ITO is efficient in retaining enzyme activity and the cholesterol biosensor has a good reproducibility.

The shelf life of ChEt-ChOx/Ufm-Cu_2O-CS/ITO bioelectrode (Figure 8D) has been monitored by amperometric measurement in the presence of 100 mg/dL standard cholesterol oleate solution in PBS at a regular interval of 1 day up to 15 days and then after an interval of 15 days. It has been found that the bioelectrode retains its enzyme activity up to 97% after 15 days, 94% after 30 days, and 89% after 45 days and falls to 82% after 60 days of its original response current, showing a longer lifetime when stored under refrigerated condition (4 °C). The good stability may perhaps be due to the fact that the Ufm-Cu_2O-CS matrix provides an appropriate microenvironment for retaining the bioactivity of the enzyme molecules.

Application of ChEt-ChOx/Ufm-Cu_2O-CS/ITO Bioelectrode for the Determination of Total Cholesterol in Human Blood Serum Sample. To demonstrate clinical application of the biosensor, we have assayed serum samples. The serum samples and their cholesterol concentrations have been provided by a local medical examination center located in New Delhi, India. The electrochemical response current is measured in both serum and standard sample in the presence of PBS (50 mM, pH 7.0, 0.9% NaCl) containing $[Fe(CN)_6]^{3-/4-}$ (5 mM) at the 30 mV/s scan rate. The magnitudes of current obtained with serum samples and prepared standard cholesterol oleate solution are in acceptable agreement (Figure 8E), indicating that the fabricated biosensor can be used for precise determination of total cholesterol in real clinical samples. As can be seen from Table 2, the results are satisfactory and were in agreement with those measured by the serum as well as standard solution with the relative standard deviation ranging from 0.5 to 5.0%.

CONCLUSIONS

In summary, a simple electrochemical deposition method has been used for fabricating ultrafine monodispersed Cu_2O-chitosan-modified electrode that can be employed for amperometric sensing of total cholesterol. The wide detection range of 10−450 mg/dL, high sensitivity of 0.895 μA/(mg/dLcm^{-2}), and fast response time of 2s may be assigned to the enhanced current response arising due to presence of the highly catalytic Cu_2O nanoparticles in chitosan matrix, and its good biocompatibility behavior maintains the biological activity of the enzymes and facilitates electron transfer produced in the enzymatic reaction. When these superior performance characteristics are combined with long-term stability, good reproducibility, and excellent specificity to cholesterol in the presence of common interferents, the ChEt-ChOx/Ufm-Cu_2O-CS/ITO bioelectrode is a potential platform for determination of total cholesterol in human serum samples. The results clearly suggest that antimicrobial and biocompatible Ufm-Cu_2O-CS nanobiocomposite is a promising platform for the development of other in vitro and in vivo biosensors and bioelectronic devices and investigation of electrochemistry at functionalized interfaces.

ASSOCIATED CONTENT

Supporting Information

Antimicrobial activity test and bioassay of Cu_2O/CS, ChEt-ChOx/Ufm-Cu_2O/CS, and CS solution against at different microorganisms/algae/fungi. Magnitude of potential difference as a function of scan rate (10−100 mV/s) and effect of working potential in the range of 0.1 to 0.8 V on the performance of the ChEt-ChOx/Cu_2O-CS bioelectrode. The effect of interferents on the electrctrochemical response of the ChEt-ChOx/Ufm-Cu_2O-CS/ITO bioelectrode. This material is available free of charge via the Internet at http://pubs.acs.org.

AUTHOR INFORMATION

Corresponding Author

*Phone: +91-11-27294668. Fax: 91-11-2787102. E-mail: bansi.malhotra@gmail.com.

Notes

The authors declare no competing financial interest.

■ ACKNOWLEDGMENTS

We thank Director, National Physical Laboratory, New Delhi, India for providing the facilities. J.S. thanks World Class University (WCU) program (R31-20029) funded by MEST, Republic of Korea for providing financial support. We thank Prof. Radha Prasanna and Ms. Vidhi Chaudhary (IARI, New Delhi, India) for interesting discussions relating to biocompatibility studies. B.D.M. thanks the Ministry of Education, Science and Technology (R32-20026) of Korea for the opportunity provided during his visit to the Chungnam National University as visiting professor under the World Class University project during June−July 2012.

■ REFERENCES

(1) Nauck, M.; Marz, W.; Wieland, H. *Clin. Chem.* **2000**, *46*, 436−437.
(2) Malhotra, B. D.; Chaubey, A. *Sens. Actuators, B* **2003**, *91*, 117−127.
(3) Monosık, R.; Stredansky, M.; Sturdık, E. *J. Clin. Lab. Anal.* **2012**, *26*, 22−34.
(4) Arya, S. K.; Datta, M.; Malhotra, B. D. *Biosens. Bioelectron.* **2008**, *23*, 1083−1100.
(5) Gopalan, A. I.; Lee, K. P.; Ragupathy, D. *Biosens. Bioelectron.* **2009**, *24*, 2211−2217.
(6) Ahmadalinezhad, A.; Chen, A. *Biosens. Bioelectron.* **2011**, *26*, 4508−4513.
(7) Kerman, K.; Saito, M.; Yamamura, S.; Takamura, Y.; Tamiya, E. *Trends Anal. Chem.* **2008**, *27*, 585−592.
(8) Wang, J. *J. Pharm. Biomed. Anal.* **1999**, *19*, 47−53.
(9) Safavia, A.; Farjamia, F. *Biosens. Bioelectron.* **2011**, *26*, 2547−2552.
(10) Ansari, A. A.; Kaushik, A.; Solanki, P. R.; Malhotra, B. D. *Electrochem. Commun.* **2008**, *10*, 1246−1249.
(11) Singh, J.; Kalita, P.; Singh, M. K.; Malhotra, B. D. *Appl. Phy. Lett.* **2011**, *98*, 123702.
(12) Cheng, F.; Jishan, H.; Zhencheng, C. *Sens. Actuators, B* **2011**, *155*, 545−550.
(13) Singh, S.; Singhal, R.; Malhotra, B. D. *Anal. Chim. Acta* **2007**, *582*, 335−343.
(14) Gupta, M. N.; Kaloti, M.; Kapoor, M.; Solanki., K. *Artif. Cells, Blood Substitutes, Immobilization Biotechnol.* **2011**, *39*, 98−109.
(15) Ansari, S. A.; Husain, Q. *Biotechnol. Adv.* **2012**, *30*, 512−523.
(16) Sassolas, A.; Blum, L. J.; Leca-Bouvier, B. D. *Biotechnol. Adv.* **2012**, *30*, 489−511.
(17) Bornscheuer, U. T. *Angew.Chem., Int. Ed.* **2003**, *42*, 3336−3337.
(18) Nguyen, T. K. T.; Luke, A. W. G. *Nano Today* **2010**, *5*, 213−230.
(19) Wang, X.; Hu, C.; Liu, H.; Du, G.; He, X.; Xi, Y. *Sens. Actuators, B* **2010**, *144*, 220−225.
(20) Liu, Y. L.; Liu, Y. C.; Mu, R.; Yang, H.; Shao, C. L.; Zhang, J. Y.; Lu, Y. M.; Shen, D. Z.; Fan, X. W. *Semicond. Sci. Technol.* **2005**, *20*, 44−49.
(21) Borgohain, K.; Murase, N.; Mahamuni, S. *J. Appl. Phy.* **2002**, *92*, 1292−1298.
(22) Li, C.; Su, Y.; Zhang, S.; Lv, X.; Xia, H.; Wang, Y. *Biosens. Bioelectron.* **2010**, *26*, 903−907.
(23) Zhu, H.; Wang, J.; Xu, G. *Cryst. Growth Design* **2009**, *9*, 633−638.
(24) Gao, Z.; Liu, J.; Chang, J.; Wu, D.; He, J.; Wang, K.; Xu, F.; Jiang, K. *Cryst. Eng. Commun* **2012**, *14*, 6639−6646.
(25) Zhang, X.; Wang, G.; Zhang, W.; Wei, Y.; Fang, B. *Biosens. Bioelectron.* **2009**, *24*, 3395−3598.
(26) Luo, X.; Morrin, A.; Killard, A. J.; Smyth, M. R. *Electroanalysis* **2006**, *18*, 319−326.
(27) Chopra, N.; Gavalas, V. G.; Bachas, L. G.; Hinds, B. J.; Bachas, L. G. *Anal. Lett.* **2007**, *40*, 2067−2096.
(28) Wanekaya, A. K.; Chen, W.; Myung, N. V.; Mulchandani, A. *Electroanalysis* **2006**, *18*, 533−550.
(29) Pandey, P.; Datta, M.; Malhotra, B. D. *Anal. Lett.* **2008**, *41*, 159−209.
(30) Lin, J.; Qu, W.; Zhang, S. *Anal. Biochem.* **2007**, *360*, 288−293.
(31) Singh, J.; Srivastava, M.; Kalita, P.; Malhotra, B. D. *Process Biochem.* **2012**, *47*, 2189−2198.
(32) Scouten, W. H.; Luong, J. H. T.; Brown, R. S. *Trends Biotechnol.* **1995**, *13*, 178−185.
(33) Renato, S. F.; Christiana, A. P.; Lucilene, D. M.; Lauro, T. K. *J. Braz. Chem. Soc.* **2003**, *14*, 230−243.
(34) Das, M.; Dhand, C.; Sumana, G.; Srivastava, A. K.; Nagarajan, R.; Lata, N. L.; Iwamoto, M.; Manaka, T.; Malhotra, B. D. *Biomacromolecules* **2011**, *12*, 540−547.
(35) Dhyani, H.; Ali, Md. A.; Pandey, M. K.; Malhotra, B. D.; Sen, P. *J. Mater. Chem.* **2012**, *22*, 4970−4976.
(36) Zhu, H. T.; Zhang, C. Y.; Yin, Y. S. *J. Cryst. Growth* **2004**, *270*, 722−728.
(37) Zhang, H. X.; Siegert, U.; Liu, R.; Cai, W. B. *Nanoscale Res Lett* **2009**, *4*, 705−708.
(38) Zhang, W.; Shi, L.; Tang, K.; Dou, S. *Eur. J. Inorg. Chem.* **2010**, *2010*, 1103−1109.
(39) Kooti, M.; Matouri, L.; Transaction, F. *Nanotechnology* **2010**, *17*, 73−78.
(40) Zhang, H. L.; Zou, X. Z.; Lai, G. S.; Han, D. Y.; Wang, F. *Electroanalysis* **2007**, *19*, 1869−1874.
(41) Topoglidis, E.; Astuti, Y.; Duriaux, F.; Gratzel, M.; Durrant, J. R. *Langmuir* **2003**, *19*, 6894−6900.
(42) Kennedy, J. F.; White, C. A. In *Handbook of Enzyme Biotechnology*, 2nd ed.; Wiseman, A.; John Wiley & Sons: New York, 1985; pp 147−201.
(43) Lewis, J. A. *J. Am. Ceram. Soc.* **2000**, *83*, 2341−2359.
(44) Khan, R.; Kaushik, A.; Solanki, P. R.; Ansari, A. A.; Pandey, M. K.; Malhotra, B. D. *Anal. Chim. Acta* **2008**, *616*, 207−213.